Supporting information

High Proton-Conducting Mixed Proton-Transferred $[(H_2PO_4^-)(H_3PO_4)]_\infty$ Networks Supported by 2,2'-Diaminobithiazolium in Crystals

Guohao Yuan, Takashi Takeda, Norihisa Hoshino, and Tomoyuki Akutagawa*

[†]Graduate School of Engineering, Tohoku University, Sendai 980-8579, Japan and [‡]Institute of Multidisciplinary Research for Advanced Materials (IMRAM), Tohoku University, 2-1-1 Katahira, Aoba-ku, Sendai 980-8577, Japan.

E-mail akutagawa@tohoku.ac.jp

Contents

Table S1. Elemental analyses of five **DABT** salts.

Entry	Formula	Calcd.	Found
(**2,5-DABT**$^{2+}$) ($H_2PO_4^-$)$_2$	$C_6H_{12}N_4O_8P_2S_2$	C 18.28, H 3.07, N 14.21	C 18.24, H 3.24, N 13.75
(**2,5-DABT**$^{2+}$) ($H_2PO_4^-$)$_2$(H_3PO_4)$_2$	$C_6H_{18}N_4O_{16}P_4S_2$	C 12.21, H 3.07, N 9.49	C 12.49, H 3.01, N 9.58
(**2,4-DABT**$^{+}$) ($H_2PO_4^-$)	$C_6H_9N_4O_4P_4S_2$	C 24.33, H 3.06, N 18.91	C 24.32, H 3.03, N 18.73
(**2,4-DABT**$^{2+}$) ($H_2PO_4^-$)$_2$	$C_6H_{12}N_4O_8P_2S_2$	C 18.28, H 3.07, N 14.21	C 18.36, H 3.09, N 14.13
(**2,4-DABT**$^{2+}$) ($H_2PO_4^-$)$_2$(H_3PO_4)$_2$	$C_6H_{18}N_4O_{16}P_4S_2$	C 12.21, H 3.07, N 9.49	C 12.38, H 3.05, N 9.53

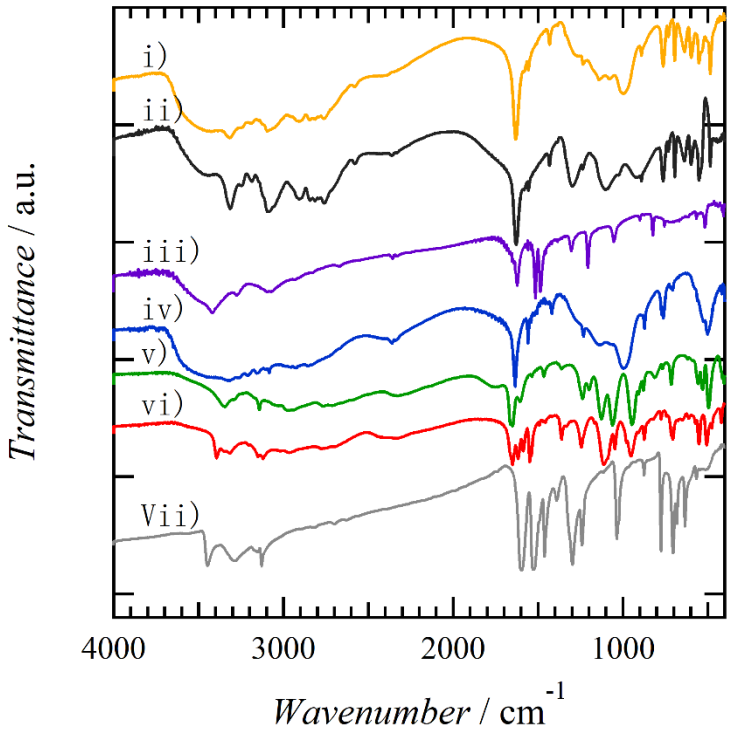

Figure S1. Vibrational IR spectra of 5 salts and **DABT** on KBr pellets. i) (**2,5-DABT**$^{2+}$)($H_2PO_4^-$)$_2$(H_3PO_4)$_2$, ii) (**2,5-H2DABT**$^{2+}$)(H_2PO4^-)$_2$, iii) **2,5-DABT**, iv) (**2,4-HDABT**$^{+}$)($H_2PO_4^-$), v) (**2,4-H2DABT**$^{2+}$)($H_2PO_4^-$)$_2$(H_3PO_4)$_2$, vi) (**2,4-H2DABT**$^{2+}$)($H_2PO_4^-$)$_2$, and vii) **2,4-DABT**.

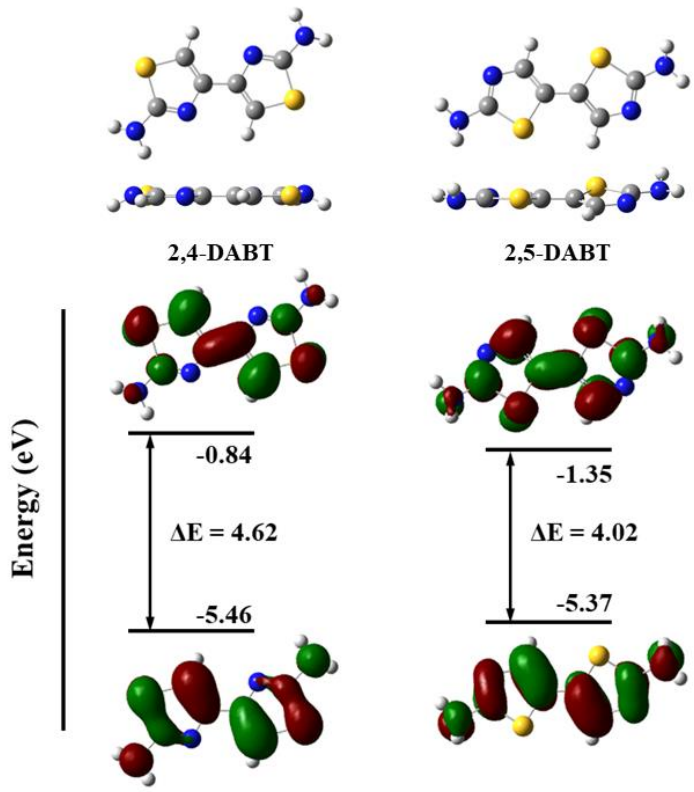

Figure S2. Molecular orbital and energy levels of the HOMO and LUMO of **2,4-DABT** and **2,5-DABT** based on the DFT calculation of a B3LYP/6-31G (d).

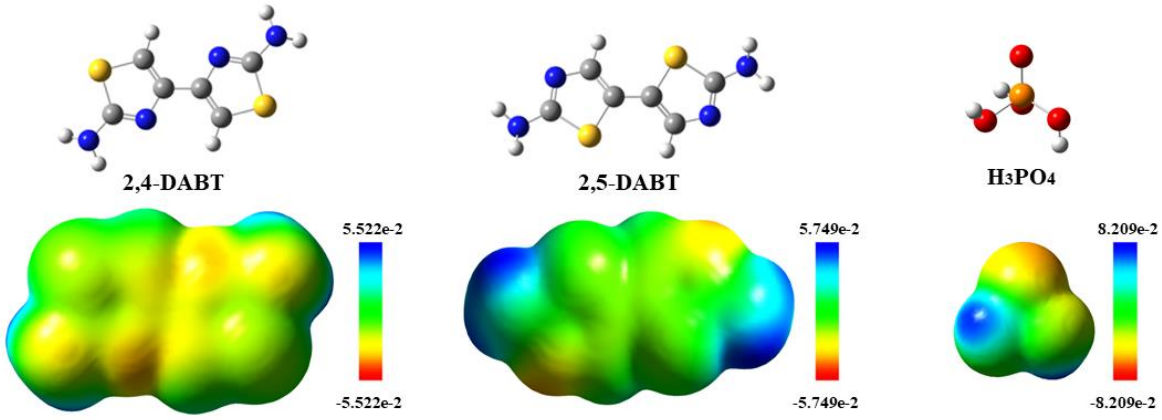

Figure S3. Electrostatic potential map (ESP) of **2,4-DABT**, **2,5-DABT**, and **H_3PO_4** based on the DFT calculation of a B3LYP/6-31G (d).

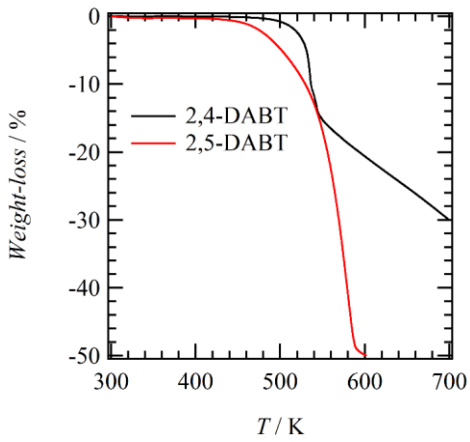

Figure S4. TG charts of **2,4-DABT** and **2,5-DABT** crystals.

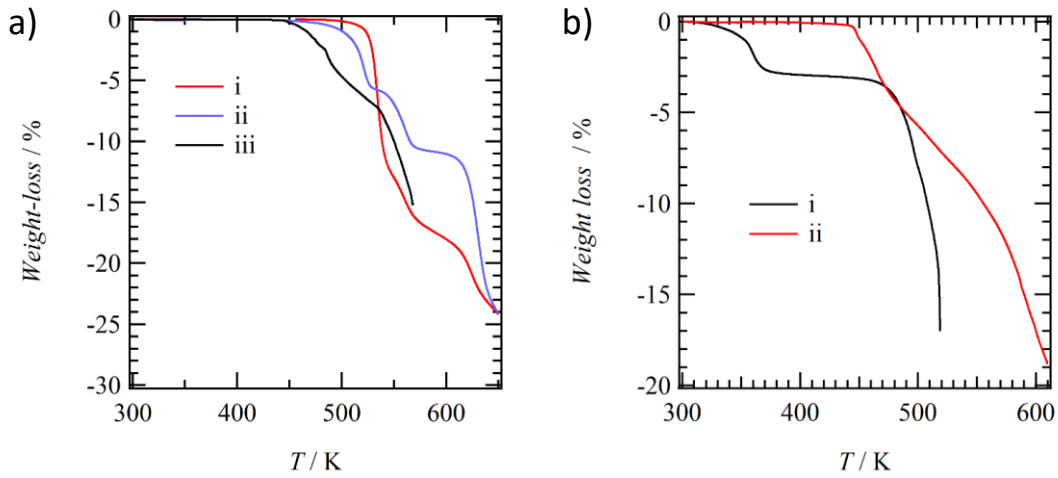

Figure S5. TG charts of **2,4-DABT** and **2,5-DABT** salts with H_3PO_4. a) **2,4-DABT** salts of i) (**2,4-HDABT**$^{+}$)($H_2PO_4^-$), ii) (**2,4-H2DABT**$^{2+}$)($H_2PO_4^-$)$_2$, and iii) (**2,4-H2DABT**$^{2+}$)($H_2PO_4^-$)$_2$(H_3PO_4)$_2$. b) **2,5-DABT** salts of i) (**2,5-H2DABT**$^{2+}$)($H_2PO_4^-$)$_2$ and ii) (**2,5-H2DABT**$^{2+}$)($H_2PO_4^-$)$_2$(H_3PO_4)$_2$.

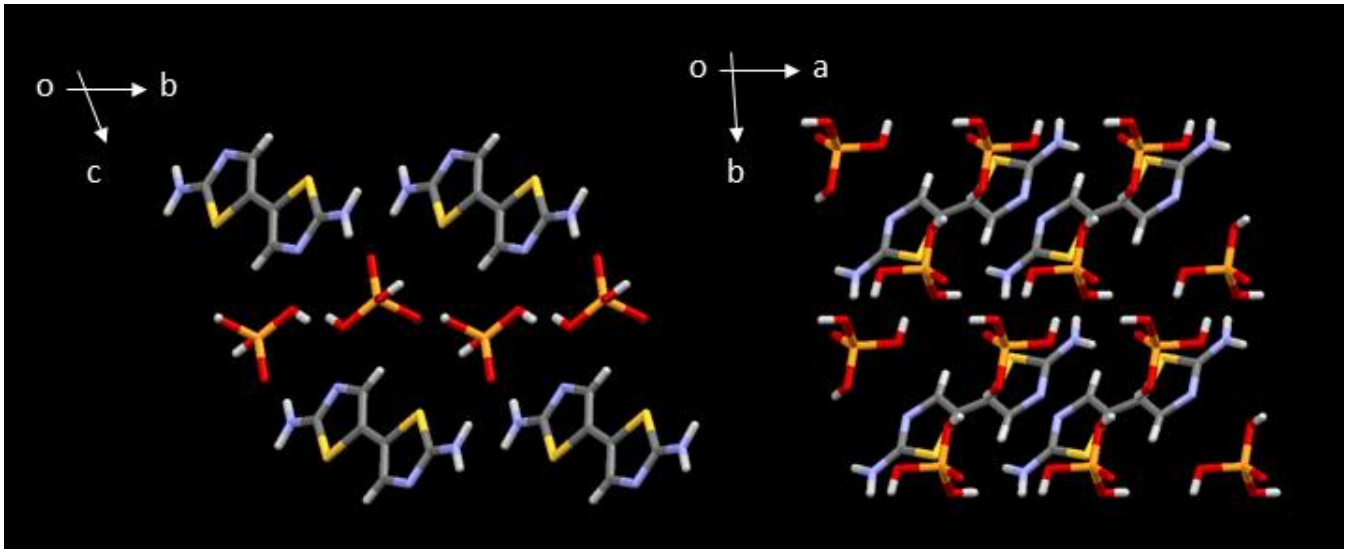

Figure S6. Crystal structure of **(2,5-DABT^{2+})**$(H_2PO_4^-)_2$

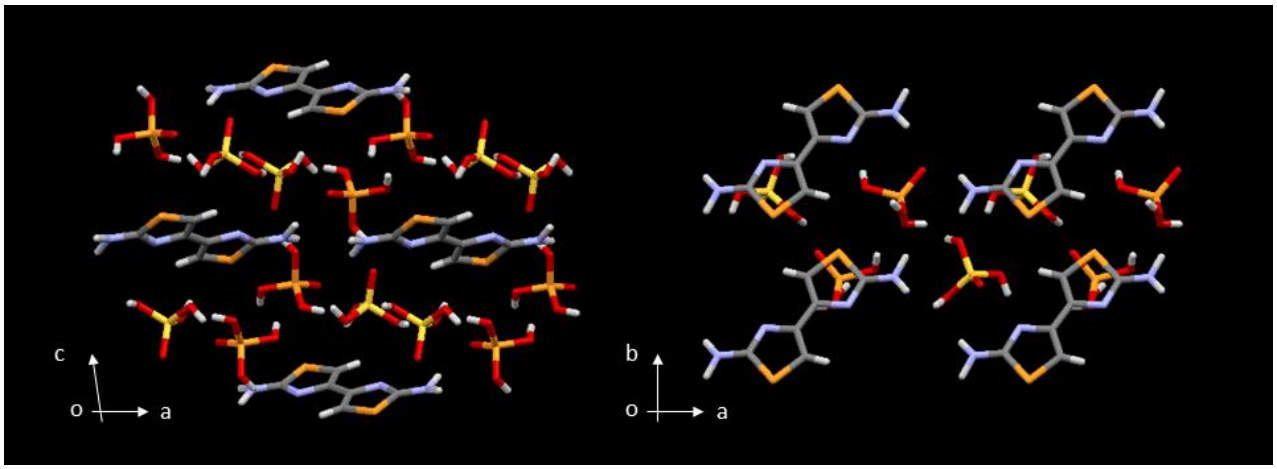

Figure S7. Crystal structure of (**2,4-DABT^{2+}**)$(H_2PO_4^-)_2(H_3PO_4)_2$

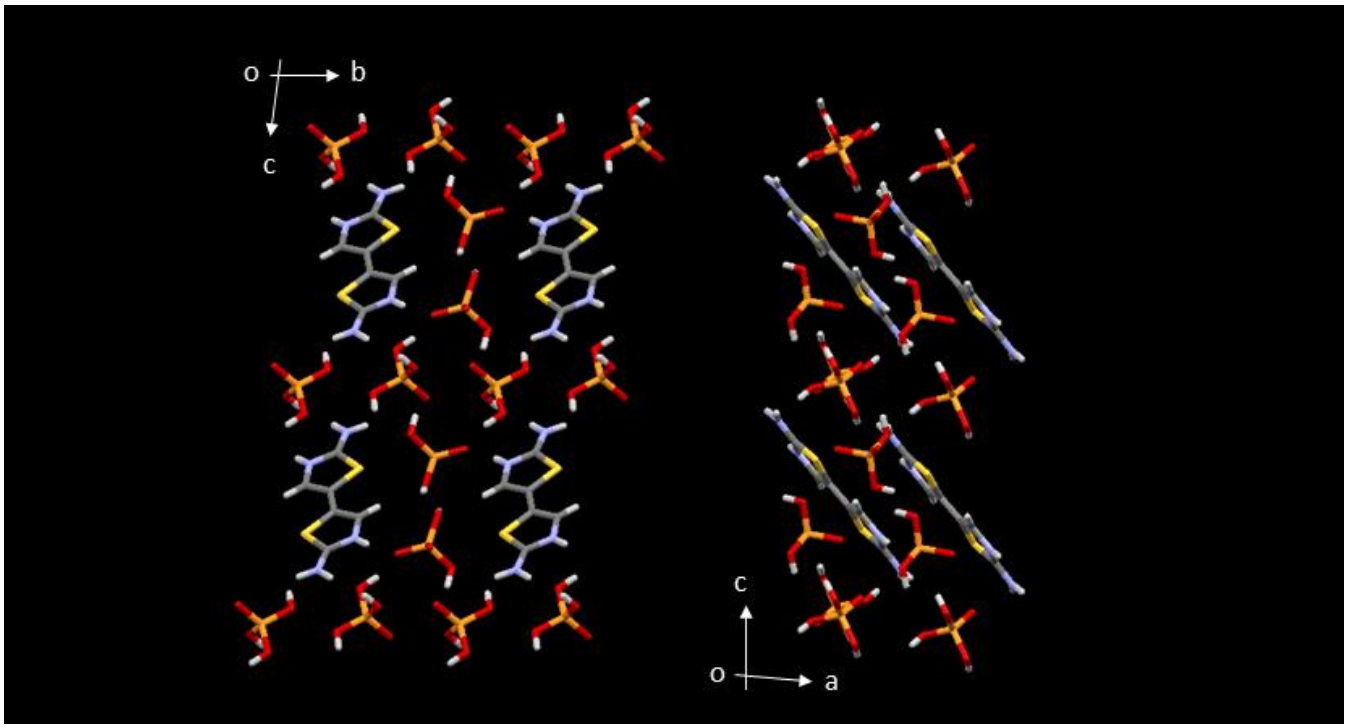

Figure S8. Crystal structure of (**2,5-DABT**$^{2+}$)($H_2PO_4^-$)$_2$(H_3PO_4)$_2$

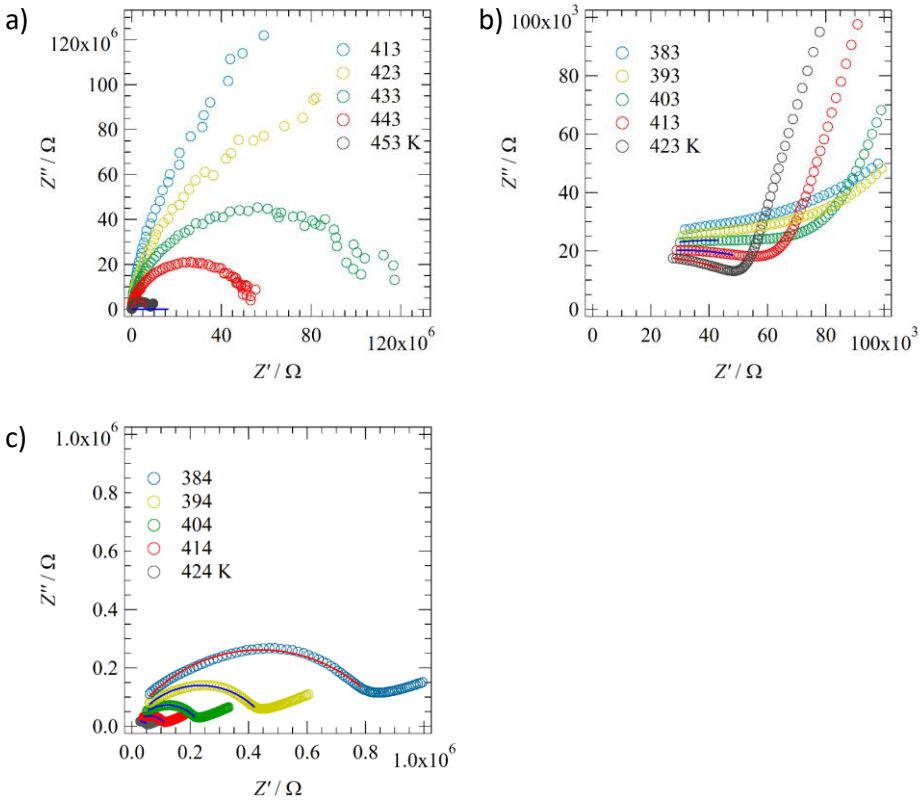

Figure S9. Temperature-dependent *Z*'-*Z*'' plots of a) (**2,4-HDABT**$^{+}$)($H_2PO_4^-$), b) (**2,4-H2DABT**$^{2+}$)($H_2PO_4^-$)$_2$, and c) (**2,4-H2DABT**$^{2+}$)($H_2PO_4^-$)$_2$(H_3PO_4)$_2$ using the compressed pellets. Protonic conductivities of each crystal were determined by the semicircles using below equation.

$$z'' = \sqrt{\left(\frac{R}{2}\right)^2 - \left(z' - \frac{R}{2}\right)^2} \qquad \text{eq. S1}$$

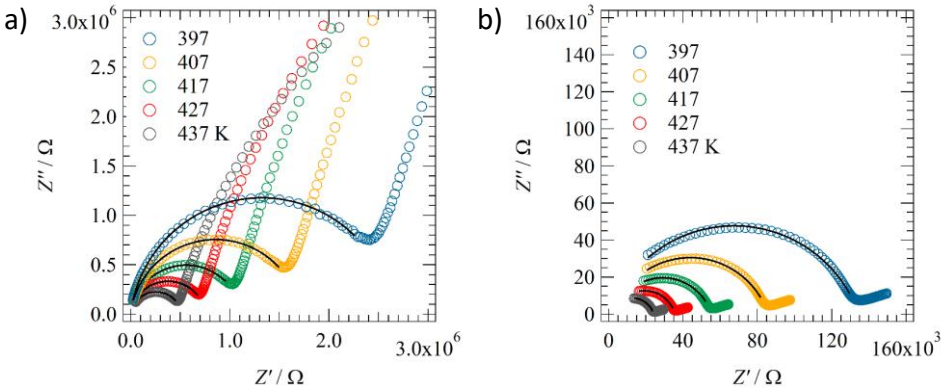

Figure S10. Temperature-dependent *Z*'-*Z*'' plots of a) (**2,5-H2DABT**$^{2+}$)($H_2PO_4^-$)$_2$ and b) (**2,5-H2DABT**$^{2+}$)($H_2PO_4^-$)$_2$(H_3PO_4)$_2$ using the compressed pellets.

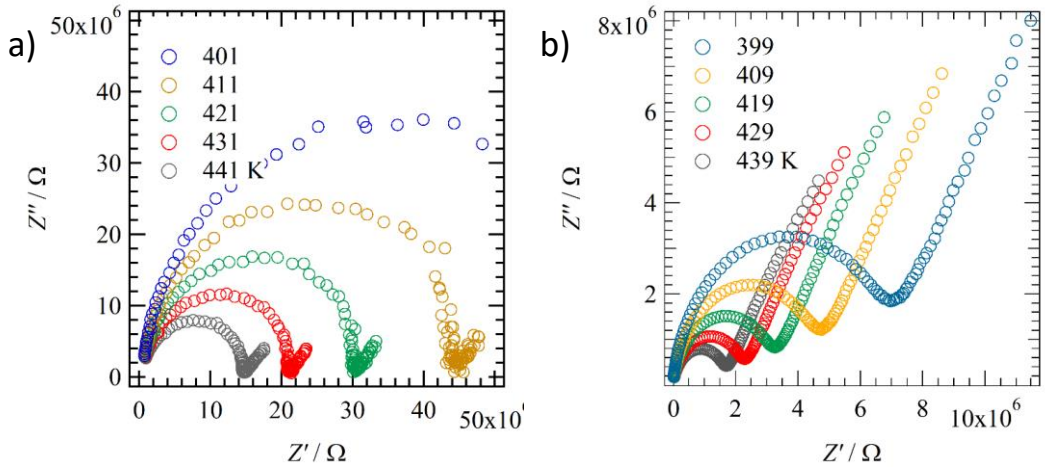

Figure S11. Temperature-dependent *Z*'-*Z*'' plots of single crystal of (**2,4-H2DABT**$^{2+}$)($H_2PO_4^-$)$_2$ a) along the *c*-axis and b) along the *b*-axis.

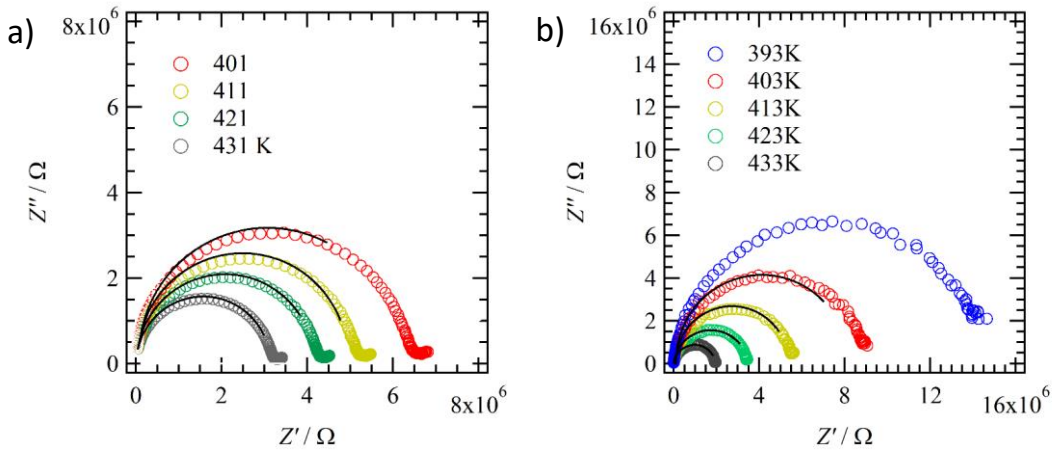

Figure S12. Temperature-dependent *Z*'-*Z*'' plots of single crystal of (**2,4-H2DABT**$^{2+}$)($H_2PO_4^-$)$_2$(H_3PO_4) a) along the *b*-axis and b) along the *a*+*c* axis.

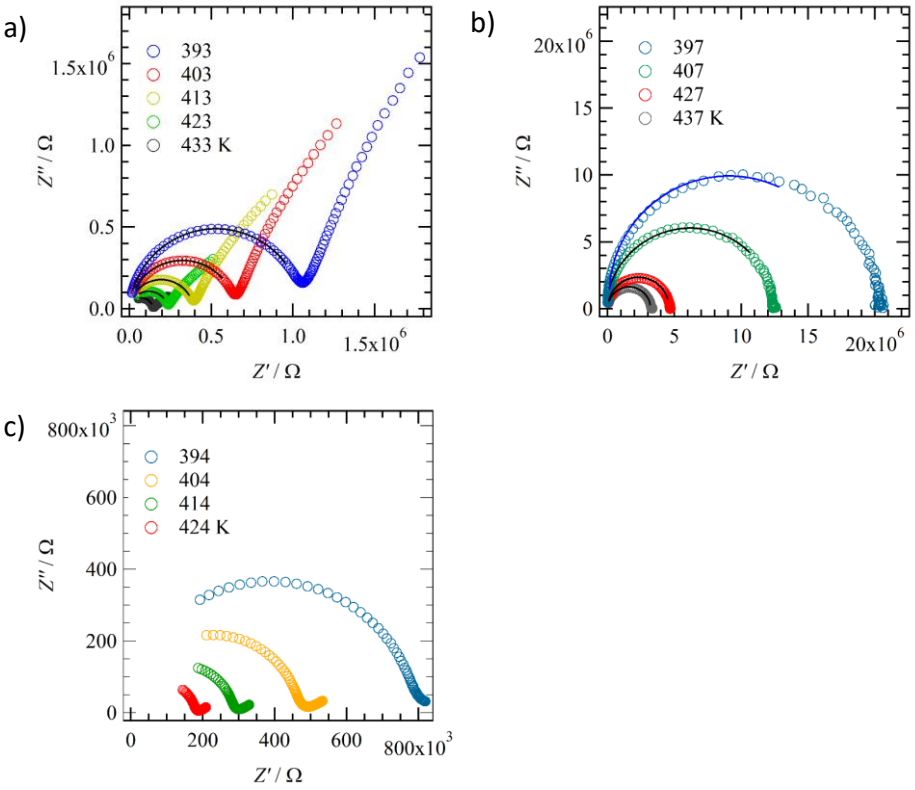

Figure S13. Temperature-dependent *Z*'-*Z*'' plots of single crystal of (**2,5-H2DABT**$^{2+}$)($H_2PO_4^-$)$_2$(H_3PO_4) a) along the *c*-axis, b) along the *b*-axis, and b) along the *c*-axis.

Table S2. The proton conductivities in each measurement temperature.

Compound		*T*, K				
		σ, S cm^{-1}				
(**2,5-H2DABT^{2+}**)	Powder	437	427	417	407	397
$(H_2PO_4^-)_2$		7.1×10^{-6}	4.8×10^{-6}	3.3×10^{-6}	2.1×10^{-6}	1.4×10^{-6}
	[010]	439	429	419	409	
		1.2×10^{-5}	8.7×10^{-6}	6.9×10^{-6}	4.2×10^{-6}	
	[001]	441	431	421	411	401
		2.6×10^{-6}	1.96×10^{-6}	1.5×10^{-6}	1.0×10^{-6}	6.8×10^{-7}
(**2,5-H2DABT^{2+}**)	Powder	437	429	419	409	399
$(H_2PO_4^-)_2\,(H_3PO_4)_2$		2.6×10^{-5}	1.7×10^{-5}	1.1×10^{-5}	7.6×10^{-6}	5.0×10^{-6}
	[001]	434	414	404	394	
		1.9×10^{-4}	7.8×10^{-5}	5.9×10^{-5}	4.6×10^{-5}	
	[010]	437	427	407	397	
		4.5×10^{-4}	3.1×10^{-4}	1.2×10^{-4}	8.1×10^{-5}	
	[100]	433	423	413	403	393
		6.0×10^{-6}	3.7×10^{-6}	2.2×10^{-6}	1.3×10^{-6}	8.2×10^{-7}
(**2,4-HDABT^{+}**)	Powder	453	443	433		
$(H_2PO_4^-)$		8.7×10^{-9}	7.5×10^{-9}	3.1×10^{-9}		
(**2,4-H2DABT^{2+}**)	Powder	433	423	413		
$(H_2PO_4^-)_2$		6.5×10^{-6}	5.1×10^{-6}	4.0×10^{-6}		
(**2,4-H2DABT^{2+}**)	Powder	424	414	404	394	384
$(H_2PO_4^-)_2\,(H_3PO_4)_2$		1.8×10^{-5}	8.3×10^{-6}	4.2×10^{-6}	2.1×10^{-5}	1.1×10^{-5}
	[101]	431	421	411	401	
		1.6×10^{-5}	1.2×10^{-5}	1.0×10^{-5}	8.5×10^{-5}	
	[010]	433	423	413	403	393
		2.4×10^{-7}	1.4×10^{-7}	8.9×10^{-7}	5.9×10^{-7}	3.9×10^{-7}